most suitable tissues for gene gun-based DNA vaccination against infectious diseases.
© 2003 Japanese Society for Investigative Dermatology. Published by Elsevier Science Ireland Ltd. All rights reserved.

1. Introduction

The oral mucosa is exposed to a variety of environmental antigens, including dietary antigens, chemicals, and pathogenic organisms, and it is one of the first lines for host defenses against various infectious agents. The murine oral mucosa contains a network of directly accessible MHC class II^+ dendritic cells (DC), similar to skin Langerhans cells, and serves as an efficient and inductive site for local and remote immune response [1,2]. Transepithelial delivery of antigens through the oral mucosa has proven to be efficient at inducing antigen-specific cellular immune responses [3–6].

Direct immunization via mucosal surfaces has been considered for many vaccine approaches, including DNA vaccines [7,8]. Recently, DNA vaccines have shown certain advantages over other types of vaccines in terms of safety and the elicitation of antigen-specific cellular immune responses as well as humoral immune responses. Indeed, oral mucosal injection of a recombinant naked DNA plasmid encoded measles virus hemagglutinin (HA)-induced HA-specific cytotoxic T cells [4]. It remains to be determined, however, how genetic vaccination through the oral mucosa could effectively induce antigen-specific immune responses in comparison with the skin, which is generally used as the common immunization route.

A particle-mediated gene-transfer technique has been considered to be one of the most efficient methods for in vivo gene transfer, having the advantage of being simple, fast, and versatile [9–11]. A gene gun has been applied in several preclinical gene-therapy protocols [12–16].

We have recently established an oral mucosa-mediated genetic vaccination model in the hamster [6]. In this study, we compared the oral mucosal DNA vaccine in vivo and in vitro to skin vaccination, using plasmids of the influenza A/WSN/33(H1N1) hemagglutinin (HA) and the *Plasmodium berghei* circumsporozoite protein (PbCSP), respectively. Antigen-specific antibody production was not observed in each case, but IFN-γ production and cell-mediated killing activity were strongly induced in splenic lymphocytes from hamsters with the oral vaccination. Genetic immunization via the oral mucosa better protected the host hamster from the malaria parasite than the skin vaccination. These results suggest that gene immunization via the oral mucosa can more efficiently induce cell-mediated Th1 immunity than via the skin, and that it may provide a new therapeutic style of vaccination.

2. Materials and methods

2.1. Animals, cells, and plasmids

Male, 6-week-old Syrian (Golden) hamsters were purchased from SLC (Shizuoka, Japan) and maintained in the Experimental Animal Center of Jichi Medical School. These experiments were performed in accordance with the Jichi Medical School Guide for Laboratory Animals. RPMI 1846 melanoma cells were obtained from the American Type Culture Collection (Rockville, MD) and maintained in McCoy's 5a medium supplemented with 20% heat-inactivated fetal calf serum (FCS) and antibiotics [6]. MDCK cells were maintained in Dulbecco's modified Eagle's medium supplemented with medium containing 10% FCS. The cultures were kept in a 5% CO_2 and 95% air humidified atmosphere at 37 °C.

The influenza A/WSN/33(H1N1) hemagglutinin (HA) cDNA was amplified from the reading frame of HA cDNA of WSN infected MDCK cells by polymerase chain reaction (PCR) using a sense primer (5′-ATG AAG GCA AAA CTA CTG GTC CTG TTA TAT GC-3′) and an anti-sense primer (5′-TTA CCC ACA GCT GTG AAT TGA GTG TTC ATT TTC-3′). The PCR product was inserted into an expression plasmid, pcDNA3.1 vector (Invitrogen, San Diego, CA) to generate pcDNA-WSN-HA, which is expressed under the control of a CMV promoter. The plasmids, pcDNA-CS87 and phGFP-105-C1, which have been described previously [6,17], express the malaria *Plasmodium berghei* circumsporozoite protein (PbCSP), and an enhanced type of mutant in green fluorescent protein (GFP), respectively. Large-scale preparation of plasmid DNA was performed by the alkaline lysis method, and closed circular plasmid DNA was purified by equilibrium centrifugation in CsCl-ethidium bromide gradients.

2.2. Transfection and immunostaining

To establish cell lines that stably express the influenza A/WSN/33(H1N1) HA and the malaria PbCSP, transfection of pcDNA-WSN-HA or pcDNA-CS87 into RPMI 1846 cells (5×10^5 cells in a 60-mm plate) was performed using Lipofectamine 2000 Reagent (Gibco/BRL, Gaithersburg, MD). Cells were maintained with McCoy's 5a supplemented with 20% FCS for 2 days, followed by the medium containing G418 geneticine (Gibco/BRL) (600 μg/ml) for 14 days. Geneticine-resistant clones were isolated and used for cell-mediated killing assays. Similarly, lacZ transfectants (pcDNA-lacZ) were also isolated.

For the immunostaining, stable transfectants growing in cover slips were fixed with a mixture of acetone and methanol (volume ratio 3:2) and blocked with 3% bovine serum albumin in phosphate-buffered saline (PBS). The pcDNA-WSN-HA-transfected cells were incubated with MEM/ALB (Gibco/BRL) followed by rabbit anti-influenza WSN antibodies, then followed by the secondary goat anti-rabbit IgG-FITC conjugate. For the staining of *P. berghei* circumsporozoite, mouse anti-PbCSP IgG was used as the primary antibodies [17]. Stained cells were then observed using a confocal laser microscope.

2.3. Gene immunization

Gold particles coated with plasmid DNA and their cartridges were prepared as described previously [6]. The hamsters were anesthetized by an intraperitoneal route with a mixture of ketamine and xylazine (1:1) at 40 mg/body weight (kg). DNA vaccinations were performed with two kinds of DNA vaccines under the same protocol. For oral mucosa immunization, the cheek pouch of the hamster was pulled out, and DNA-coated gold particles (1 μg of plasmid DNA per shot) were delivered three times at 3-week intervals using Helios Gene Gun (Bio-Rad Laboratory, Tokyo, Japan) at 250-psi (1 psi = 6890 Pa). For skin immunization, DNA-coated gold particles were delivered three times at 3-week intervals into the shaved abdominal skin at 300-psi. Experiments were performed 2–4 times each; representative experiments are shown.

2.4. Hemagglutination inhibition test and enzyme-linked immunosorbent assay

Serum was collected by tail-vein bleeding immediately prior to each DNA bombardment, and immediately prior to in vivo challenge. For the influenza experiment, the antibody titers of each hamster were determined by a hemagglutination inhibition test (HI). For the malaria experiment, the anti-PbCSP antibodies were measured by enzyme-linked immunosorbent assay as described elsewhere [18].

For IFN-γ measurement, spleen cells were isolated from the animals 3 weeks after the final immunization, and were then stimulated in RPMI 1640 medium with 10% FCS containing 5 μg/ml of PbCSP at a concentration of 10^6 cells/ml in 200 μl at 37 °C for 48 h. Supernatants were then analyzed using ELISA kits (Genzyme, Cambridge, MA), as described in the manufacturer's instructions.

2.5. Cytotoxic T lymphocyte (CTL) assay

The CTL assay was performed 3 weeks after the final immunization (9 weeks). Spleen cells were isolated from at least three hamsters of each group. We used pcDNA-WSN-HA or pcDNA-CS87 stable transfectants as targets. Transfectants were irradiated with 80 Gy under γ-rays, and spleen cells were mixed with the irradiated cells at a 20:1 ratio for 5 days at 37 °C. The effector spleen cells were then collected and incubated with target cells at 37 °C for 5 h. The supernatant was isolated and examined by lactate dehydrogenase release (Cytotoxicity Detection Kit: Roche, Germany). The percent cytotoxicity was calculated as follows: cytotoxicity (%) = (experimental value − low control) × 100/(high control − low control). High control and low control were obtained by incubating the target cells either with 0.5% Triton X-100 or alone, respectively. The percent cytotoxicity is indicated as average values from assays performed in triplicate.

2.6. In vivo malaria challenge and evaluation of parasitemia

As a rodent malaria parasite, the *P. berghei* ANKA strain clone 2.34 was used. *Anopheles stephensi* Swiss 500 strain was used as a malaria vector. The preparation of infective mosquitoes has been described previously [18]. Three weeks after the final immunization, the hamsters were challenged by bites of *P. berghei*-infected *Anopheles stephensi*. Sedated hamsters were placed on a nylon-mesh screened container containing infected mosquitoes. Each hamster was removed after a minimum of five observed mosquito feedings over 5 min. We chose the bites of *P. berghei*-infected mosquitoes for challenge to emulate the natural route of malaria infection. Malaria parasites were

monitored in the peripheral blood of the hamster from day 4 after the sporozoites inoculation. Parasitemia was calculated from the actual number of parasitized red blood cells relative to approximately 2×10^4 red blood cells. Parasitemia on day 6 after in vivo challenge was compared in each group using the Mann–Whitney *U*-test. Eight animals per experimental treatment group were used for typical experiments.

2.7. Statistics

Data are presented as mean ± standard deviation (S.D.). Statistical differences between the two groups were evaluated using the unpaired Students' *t*-test. The calculations were performed with the software Statview™ (Abacus Concepts, Berkley, CA). Values of $P < 0.05$ were considered significant.

3. Results

3.1. Transduction of RPMI 1846 cells with influenza A/WSN/33(H1N1) hemagglutinin or plasmodium berghei circumsporozoite protein

As shown in our previous work, RPMI 1846 melanoma cells can be implanted into syngeneic hamsters [6]. Because this cell line could serve as a CTL target after genetic immunization, we transduced RPMI 1846 cells with either influenza A/WSN/33(H1N1) hemagglutinin (HA) or *plasmodium berghei* circumsporozoite protein (PbCSP) cDNA to evaluate their antigen-specific CTL response. As shown in Fig. 1, the antigen cDNA-transduced cell lines were specifically stained by their specific antibodies, but not by their isotype IgG or pre-immune serum. The HA antigen was expressed exclusively on the cell membrane (Fig. 1A), and the PbCS protein was expressed in the cytoplasm and on the cell membrane (Fig. 1C). The parental cells and the LacZ transfectants were not stained with these antibodies (data not shown). Their expression was not decreased without G418 geneticin for at least 1 week (data not shown).

3.2. Oral mucosa-mediated genetic vaccine predominantly induces antigen-specific CTL response in comparison with skin vaccination

We have previously shown that an irradiated cancer vaccine coupled with IL-12 cDNA into the oral mucosa versus skin can induce long-lasting IFN-γ production [6], suggesting that oral mucosal immunization may more efficiently introduce the tumor antigen-specific CTL response than the skin immunization. To examine the effects of oral mucosal genetic immunization on the CTL response, we bombarded either pcDNA-A/WSN/33-HA or pcDNA-CS87 expression plasmid into the oral mucosa or the skin three times at 3-week intervals using a gene gun. The splenic lymphocytes from immunized hamsters were used for the CTL assay. As shown in Fig. 2, both DNA vaccines via the oral mucosa strongly induced antigen-specific CTL responses compared with the skin vaccination. Antigen-specific CTL was generated at effector: target ratios of 50:1 and 25:1. Regarding the influenza A/WSN/33-HA, the induced cytotoxicity was significantly higher in the oral mucosa immunization group (23% at E/T ratio of 25:1) than the skin group (10%) ($P = 0.03$)(Fig. 2A). No CTL response was observed against cells expressing GFP. For the malaria antigen, there was a ~2-fold difference at E/T ratio of 25:1 ($P < 0.05$) in the oral mucosa immunization group (Fig. 2B). Thus, these results indicate that genetic immunization via the oral mucosa can introduce antigen-specific CTL responses more efficiently than the skin.

Furthermore, we evaluated INF-γ levels in the spleen cells after the genetic vaccination. As shown in Fig. 3, IFN-γ production was strongly induced in splenic lymphocytes from the hamster with oral vaccination of malaria PbCSP cDNA (Fig. 3A, lane 1). Compared with the skin-immunization routes (lane 3), oral mucosal immunization is the most efficient means of inducing IFN-γ production. As with the oral immunization PbCSP cDNA, the influenza HA cDNA induced IFN-γ production in the oral immunozation group (Fig. 3B), Therefore, these results suggest that oral mucosa-mediated genetic immunization can effectively mobilize cell-mediated immune response in comparison with skin-mediated vaccinations.

3.3. Serological analysis after genetic immunization

To evaluate antigen-specific antibody production after DNA vaccination, serological studies were performed using serum from immunized hamsters. For the influenza experiment, the antigen-specific antibody titers for each hamster were determined by a hemagglutination inhibition test. The titer of the specific antibody against the influenza HA antigen was beneath the level of sensitivity of the test in both the oral mucosa and skin immunization groups (data not shown). For specific-antibody

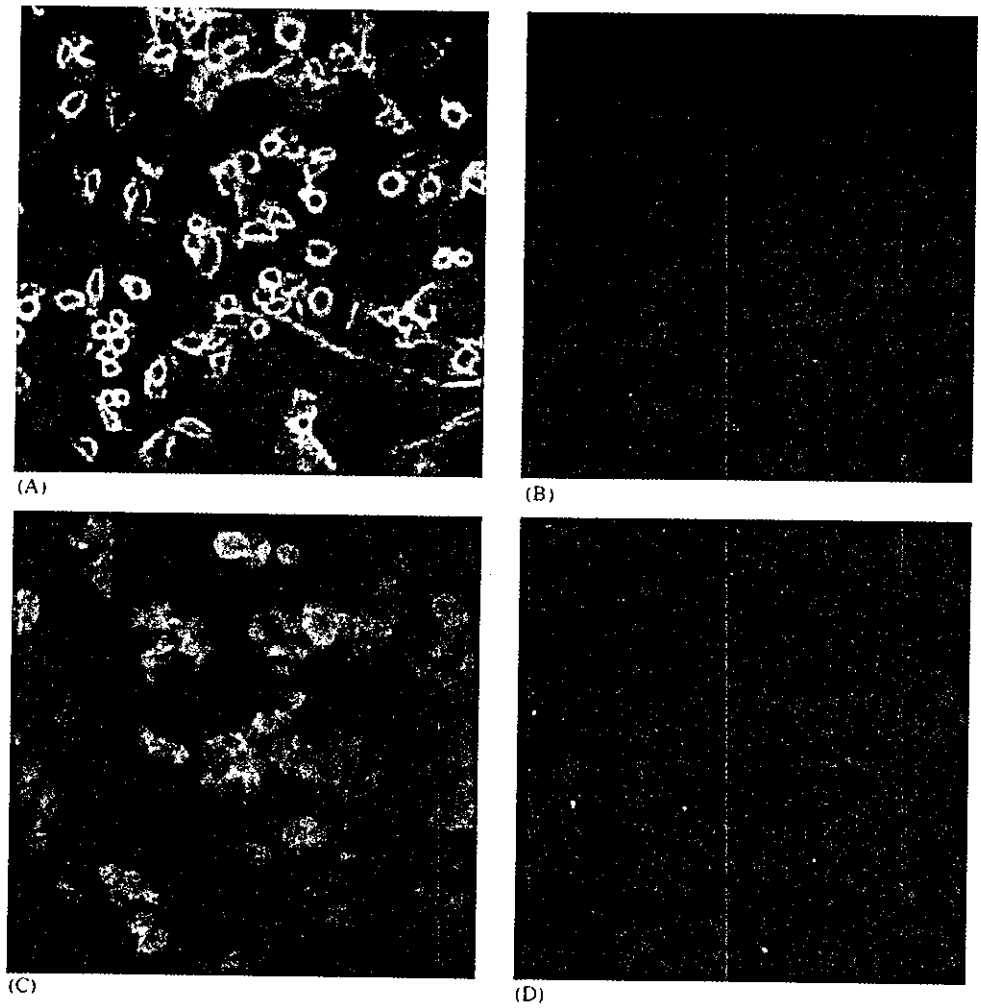

Fig. 1 Stable transduction of RPMI1846 cells with influenza A/WSN/33(H1N1) hemagglutinin or malaria *Plasmodium berghei* circumsporozoite protein cDNA. The expression plasmid of either A/WSN/33(H1N1) HA or *Plasmodium berghei* circumsporozoite protein was stably transduced into RPMI 1846 cells. Cells were fixed with a mixture of acetone and methanol (3:2) and stained with the antibodies raised against either A/WSN/33(H1N1) HA or *Plasmodium berghei* circumsporozoite protein. Stable transfectants with pcDNA-WSN-HA were stained with rabbit anti-influenza WSN antibodies (A) and with control rabbit IgG (B). Cells with pcDNA-CS87 were treated with mouse anti-PbCSP IgG (C) and normal mouse IgG (D).

production against the malaria antigen, the anti-PbCSP antibodies were also evaluated by enzyme-linked immunosorbent assay 9 weeks after the vaccination. As shown in Table 1, significant antibody production against PbCSP was not observed. These results indicate that both immunization routes using DNA vaccine cannot successfully induce antigen-specific antibody production during this period.

3.4. Protection induced by the oral mucosal vaccination against malaria challenge

We also have previously shown that liver-mediated genetic vaccination also can more effectively prevent malaria infection than skin-mediated genetic vaccination [17]. Fig. 3 also suggests that oral mucosa-mediated gene vaccination more effectively introduces a Th1-type immune response than liver-mediated vaccination. To evaluate the effects of the oral mucosal gene vaccine *in vivo*, we performed the malaria challenge after the oral gene vaccination. After the bites by *P. berghei*-infected mosquitoes, malaria parasites appeared in the peripheral blood on day 4–6 in hamsters of each group except the oral mucosal immunization group. Parasitemia in hamsters on day 6 was then compared among oral, skin, and liver immunization groups. As shown in Table 2, the oral mucosal immunization group significantly delayed the blood-appearance day of the parasites by 2 days compared with other immunization

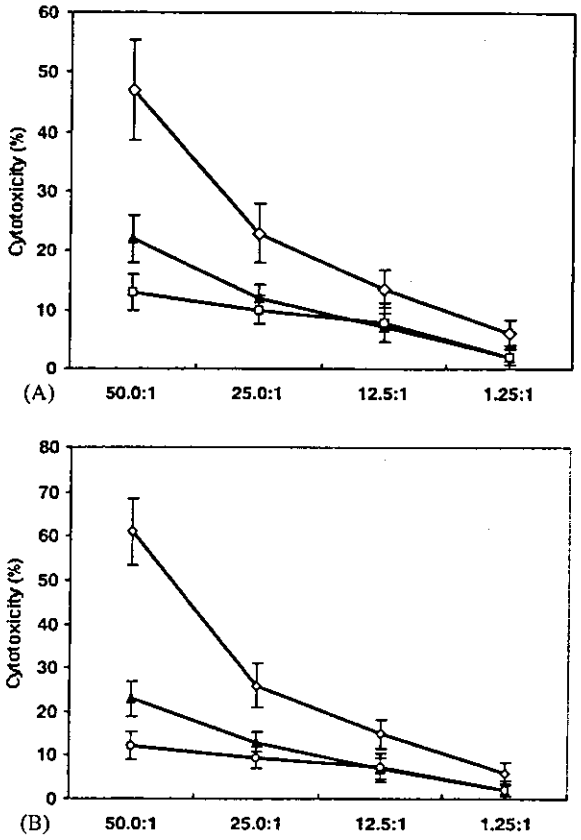

Fig. 2 Oral mucosa-mediated genetic vaccine predominantly induces antigen-specific CTL response in comparison with skin vaccination. Specific CTL activity of hamsters was evaluated in each group after DNA vaccinations. (A) For influenza HA antigen, the induced cytotoxicity (%) was markedly higher in the oral mucosa immunization group than the skin group ($P < 0.05$). ◇, pcDNA-WSN-HA into the oral mucosa; ▲, phGFP-105-C1 into the oral mucosa; ■, pcDNA-WSN-HA into the skin. Error bar, S.D. ($n = 5$). (B) In malaria antigen, the percent cytotoxicity was twofold higher in the oral mucosa immunization group than the skin group at 50:1 and 25:1 effector: target ratios ($P < 0.05$). ◇, pcDNA-CS87 into the oral mucosa; ○, phGFP-105-C1 into the oral mucosa; ▲, pcDNA-CS87 into the skin. Error bar, S.D. ($n = 6$).

groups ($P < 0.05$). In the early phase of malaria infection, parasitemia increases 10-fold per day: 1-day delay of the first blood appearance results in 90% reduction of malaria parasites. Thus, more than 90% of parasite reduction was achieved in the oral mucosal immunization group.

Taken together with the high CTL activity in oral mucosal vaccination, these results suggest that oral mucosa-mediated gene vaccination can contribute to the early phase of host protection against the malaria parasite via CTL induction.

4. Discussion

We have previously found that immunization with an irradiated melanoma vaccine into the oral mucosa can induce systemic antitumor immunity more efficiently than immunization of the skin [6]. In this study, we demonstrated that genetic vaccination using cDNA of the influenza HA and the malaria PbCSP also better introduced the antigen-specific CTL and IFN-γ production in comparison to skin- and liver-mediated vaccination. The oral mucosa was also found to be as effective an organ for particle-mediated gene transfer as the skin [6]. Our results therefore suggest that the oral mucosa may be a feasible tissue for inducing the antigen-specific CTL and Th1-type immune response against a diversity of environmental antigens.

The direct in vivo inoculation of plasmid DNA to raise immune responses represents a novel approach to vaccination. The direct inoculation of plasmid DNA encoding antigenic proteins allows the inoculated host cells to express the immunizing proteins, with neither protein purification nor a recombinant viral vector being required. The expressed proteins in the host cells result in the presentation of normally processed proteins to the immune system. This process is essential to raising immune responses against the native forms of the protein [19], resulting in an immunogen with MHC class I presentation for eliciting $CD8^+$ T-cell responses. Interestingly, in stark contrast to the oral mucosa, administration of plasmid DNA via nasal and vaginal routes has been demonstrated to induce only limited systemic immune responses [7].

Although the precise reason why vaccination of the oral mucosa is more efficient than skin immunization has yet to be elucidated, it is likely to be associated with the function of the unique immune effector cells distributed in the oral mucosa such as Langerhans cells (LC). The oral mucosa represents a unique anatomical site in which DC located in the epithelium are directly accessible to foreign antigens. Staining of the ATPase in the oral mucosa of the hamster did not show a difference in the density of LC distributed between the oral mucosa and the epidermis (data not shown). It has been reported that murine epithelial DC in the oral mucosa exhibits phenotypic, dynamic, and functional characteristics similar to those of epidermal LC [3]. The B7.2 molecule on the oral DC also may be involved in T-cell priming, as with the case of the skin DC.

Generation of antigen-specific CTL by oral mucosal immunization is not limited to genetic vaccine, but can also be induced by several types of antigens. These include haptens that are pro-

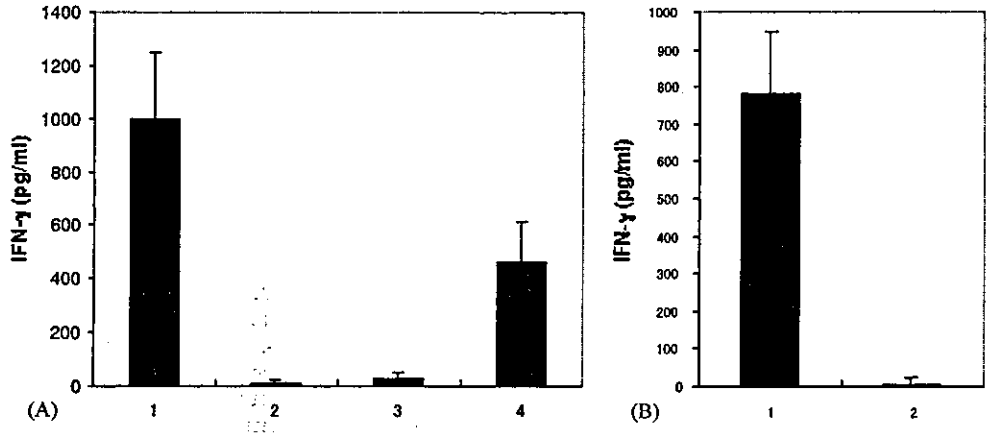

Fig. 3 Induction of IFN-γ production in splenic lymphocytes from hamster with oral vaccination of malaria PbCSP cDNA. IFN-γ levels from splenocytes were assayed by ELISA. (A) IFN-γ production was more strongly induced in hamster splenic lymphocytes via oral vaccination than via skin vaccination of malaria PbCSP cDNA ($P < 0.001$). Lane 1, administration of pcDNA-CS87 into the oral mucosa; lane 2, administration of phGFP-105-C1 into the oral mucosa, lane 3, pcDNA-CS87 into the skin; lane 4, pcDNA-CS87 into the liver. Error bar, S.D. ($n = 4$). (B) IFN-γ production with the influenza HA antigen cDNA. Lane 1, administration of pcDNA-WSN-HA into the oral mucosa; lane 2, pcDNA-WSN-HA into the skin. $P < 0.001$, error bar, S.D. ($n = 3$).

Table 1 ELISA assay of hamster serum after 9 weeks of PbCSP cDNA vaccination

Group	*n*	Vaccination/route	Absorbance (OD 405)
1	8	pcDNA-CS 87/oral	0.35 ± 0.14*
2	8	pcDNA-CS 87/skin	0.26 ± 0.17*
3	8	phGFP-105-C1/oral	0.19 ± 0.11*

* $P > 0.05$, There are no significant differences between groups.

cessed in the MHC class I pathway and induce tissue inflammation [20], recombinant plasmid DNA with immunostimulatory CpG motifs [21], and invasive recombinant adenylate cyclase toxin from *Bordetella pertussis* [22]. Indeed, these antigens have the common feature of their intrinsic adjuvant and /or proinflammatory property. Thus, foreign antigens with a unique ability to stimulate innate immunity may lead to efficient CTL responses when delivered via DC of the oral mucosa.

The study of in vivo malaria challenge suggested that oral mucosa-mediated gene vaccination contributes to the early phase of host protection against malaria parasite via CTL induction. Indeed, the protective effect from the malaria with the oral immunization did not appear to be sufficient. Parasitemia, however, will increase 10-fold a day in the early phase of malaria infection, and immediately reach to nearly a hundred percent in a short course [17]. As 1-day delay of the first blood-appearance means 90% reduction of malaria parasites, more than 90% of parasite reduction is presumably achieved in oral mucosal immunization group, and accordingly parasitemia at day 7 or 8 should differ between the oral mucosal and the skin immunization groups. Although specific antibody production may be required to achieve complete prevention, it is possible that the strong induction of T-helper type 1 (Th1) immune response via the oral mucosa may suppresse the T-helper type 2 (Th2) immune reaction, including antibody production. Based on the flexible modification with gene gun-based immunization illustrated in the present study, this problem might be thus dissolved by an altered administration schedule and/or combination with cDNA of adjuvant cytokines.

Table 2 Comparison of malaria infectivity among vaccination groups

Group	*n*	Immunization routes	Gene	Mean days of parasites appearance (range)	% parasitemia of day 6 (range)
1	8	Oral mucosa	CS 87	6.7* (6–8)	0.03* (0–0.09)
2	8	Skin	CS 87	5.0 (4–6)	0.30 (0.05–0.6)
3	8	Liver	CS 87	5.3 (5–6)	0.42 (0.02–0.8)
4	8	Oral mucosa	GFP105	4.9 (4–5)	0.33 (0.02–0.6)

* There are significant difference between group 1 and other groups (Mann–Whiney *U*-test, $P < 0.05$).

In summary, we have demonstrated that genetic immunization via the oral mucosa effectively introduces antigen-specific CTL and IFN-γ production. The oral mucosa may thus provide a novel immunization route for efficient priming of immune responses against various environmental pathogens.

Acknowledgements

We would like to thank Ms. Masako Matsumoto for her kind help with the manuscript. We also greatly appreciate the skillful technical assistance of Ms. Kyoko Okamoto and Ms. Noriko Hayashi. Jun Wang is a Ph.D. student from the first affiliated hospital of China Medical University, Shenyang, China, who is supported by the Jichi Medical School Student Fellowship. This work was supported by a grant from the Ministry of Education, Culture, Sports, Science, and Technology of Japan (No: 13470261).

References

[1] Ahlfors E, Czerkinsky C. Contact sensitivity in the murine oral mucosa. I. An experimental model of delayed-type hypersensitivity reactions at mucosal surfaces. Clin Exp Immunol 1991;86:449–56.

[2] Eriksson K, Ahlfors E, George-Chandy A, Kaiserlian D, Czerkinsky C. Antigen presentation in the murine oral epithelium. Immunology 1996;88:147–52.

[3] Desvignes C, Esteves F, Etchart N, Bella C, Czerkinsky C, Kaiserlian D. The murine buccal mucosa is an inductive site for priming class I-restricted CD8+ effector T cells in vivo. Clin Exp Immunol 1998;113:386–93.

[4] Etchart N, Buckland R, Liu MA, Wild TF, Kaiserlian D. Class I-restricted CTL induction by mucosal immunization with naked DNA encoding measles virus haemagglutinin. J Gen Virol 1997;78:1577–80.

[5] Etchart N, Desmoulins PO, Chemin K, Maliszewski C, Dubois B, Wild F, Kaiserlian D. Dendritic cells recruitment and in vivo priming of CD8+ CTL induced by a single topical or transepithelial immunization via the buccal mucosa with measles virus nucleoprotein. J Immunol 2001;167:384–91.

[6] Wang J, Murakami T, Hakamata Y, Ajiki T, Jinbu Y, Akasaka Y, Ohtsuki M, Nakagawa H, Kobayashi E. Gene gun-mediated oral mucosal transfer of interleukin 12 cDNA coupled with an irradiated melanoma vaccine in a hamster model: successful treatment of oral melanoma and distant skin lesion. Cancer Gene Ther 2001;10:705–12.

[7] Wang B, Dang K, Agadjanyan MG, Srikantan V, Li F, Ugen KE, Boyer J, Merva M, Williams WV, Weiner DB. Mucosal immunization with a DNA vaccine induces immune responses against HIV-1 at a mucosal site. Vaccine 1997;15:821–5.

[8] Ban EM, van Ginkel FW, Simecka JW, Kiyono H, Robinson HL, McGhee JR. Mucosal immunization with DNA encoding influenza hemagglutinin. Vaccine 1997;15:811–3.

[9] Pardoll DM, Beckerieg AM. Exposing the immunology of naked DNA. Immunity 1995;3:165–9.

[10] Robinson HL, Lu S, Feltquate DM, et al. DNA vaccine. AIDS Res Hum Retroviruses 1996;12:455–7.

[11] Liu MA, Hilleman MR, Kurth RE, et al. DNA vaccine: a new era in vaccinology. Ann NY Acad Sci 1995;772:291–4.

[12] Tang DC, Devit M, Johnston SA. Genetic immunization is a simple method for eliciting an immune response. Nature 1992;356:152–4.

[13] Ulmer JB, Donnelly JJ, Parker SE, et al. Heterologous protection against influenza by injection of DNA encoding a viral protein. Science 1993;259:1745–9.

[14] Davis HL, Michel ML, Whalen RG. DNA-based immunization induces continuous secretion of hepatitis B surface antigen and high level of circulating antibody. Hum Mol Genet 1993;2:1847–51.

[15] Zarozinski CC, Fynan EF, Selin LK, Robinson HL, Welsh RM. Protective CTL-dependent immunity and enhanced immunopathology in mice immunized by particle bombardment with DNA encoding an internal virion protein. J Immunol 1995;154:4010–7.

[16] Robinson HL, Hunt LA, Webster RG. Protection against a lethal influenza virus challenge by immunization with a hemagglutin-expressing plasmid DNA. Vaccine 1993;11:957–60.

[17] Yoshida S, Kashiwamura SI, Hosoya Y, Luo E, Matsuoka H, Ishii A, Fujimura A, Kobayashi E. Direct immunization of malaria DNA vaccine into the liver by gene gun protects against lethal challenge of *Plasmodium berghei* sporozoite. Biochem Biophys Res Commun 2000;271:107–15.

[18] Matsuoka H, Yoshida S, Hirai M, Ishii A. A rodent malaria, *plasmodium berghei*, is experimentally transmitted to mice by merely probing of infective mosquito, *Anopheles stephensi*. Parasitol Int 2002;51:17–23.

[19] Chen SC, Fynan EF, Robinson HL, Lu S, Greenberg HB, Santoro JC, Herrmann JE. Protective immunity induced by rotavirus DNA vaccines. Vaccine 1997;15:899–902.

[20] Kehren J, Desvignes C, Krasteva M, Ducluzeau MT, Assossou O, Horand F, Hahne M, Kagi D, Kaiserlian D, Nicolas JF. Cytotoxicity is mandatory for CD8(+) T cell-mediated contact hypersensitivity. J Exp Med 1999;189:779–86.

[21] Beyer JC, Chebloune Y, Mselli-Lakhal L, Hotzel I, Kumpula-McWhirter N, Cheevers WP. Immunization with plasmid DNA expressing the caprine arthritis-encephalitis virus envelope gene: quantitative and qualitative aspects of antibody response to viral surface glycoprotein. Vaccine 2001;19:1643–51.

[22] Walker MJ, Rohde M, Timmis KN, Guzman CA. Specific lung mucosal and systemic immune responses after oral immunization of mice with Salmonella typhimurium aroA, Salmonella typhi Ty21a, and invasive Escherichia coli expressing recombinant pertussis toxin S1 subunit. Infect Immun 1992;60:4260–8.

Available online at www.sciencedirect.com
SCIENCE DIRECT®

Microbiol. Immunol., 47(11), 841–847, 2003

Mycobacterial Infection in MyD88-Deficient Mice

Isamu Sugawara*[,1], Hiroyuki Yamada[1], Satoru Mizuno[1], Kiyoshi Takeda[2], and Shizuo Akira[2]

[1]*Mycobacterial Reference Center, The Research Institute of Tuberculosis, Kiyose, Tokyo 204–0022, Japan, and* [2]*Department of Host Defense, Research Institute for Microbial Diseases, Osaka University, Suita, Osaka 565–0871, Japan*

Received May 12, 2003; in revised form, August 11, 2003. Accepted August 13, 2003

***Abstract*: MyD88 is an adaptor protein that plays a major role in TLR/IL-1 receptor family signaling. To understand the role of MyD88 in the development of murine tuberculosis *in vivo*, MyD88 knockout (KO) mice aerially were infected with *Mycobacterium tuberculosis*. Infected MyD88 mice were not highly susceptible to *M. tuberculosis* infection, but they developed granulomatous pulmonary lesions with neutrophil infiltration which were larger than those in wild-type (WT) mice ($P<0.01$). The pulmonary tissue levels of mRNA for iNOS and IL-18 were slightly lower, but levels of mRNA for IL-1β, IL-2, IL-4, IL-6, IL-10, IFN-γ, and TGF-β were higher in MyD88 KO mice. IFN-γ, TNF-α, IL-1β, and IL-12 also were high in the sera of MyD88 KO mice. There were no statistically significant differences in the expression of TNF-α, IL-12, and ICAM-1 mRNA between MyD88 KO and WT mice. Thus, MyD88 deficiency did not influence the development of murine tuberculosis. NF-κB activity was similar in the alveolar macrophages from the lung tissues of MyD88 KO and WT mice. Also, there may be a TLR2-specific, MyD88-independent IL-1 receptor/TLR-mediated pathway to activate NF-κB in the host defense against mycobacterial infection.**

***Key words*: *Mycobacterium tuberculosis*, MyD88, MyD88 knockout mouse, NF-κB**

MyD88 originally was isolated as a myeloid differentiation primary response gene and has been shown to act as an adaptor molecule that plays an important role in TLR/IL-1 receptor/IL-18 receptor signaling (1, 2, 10). As shown previously (13, 14, 21–23), IL-1, IL-18, and TLR2 play important roles in the host defense against mycobacterial infection, which results in NF-κB activation. It also has been reported that NF-κB plays a critical role in the defense against murine tuberculosis (24). It may be that MyD88 function is closely connected to defense against bacterial infection. MyD88-deficient mice are very susceptible to *Staphylococcus aureus* infection (19), and MyD88 is required for resistance to *Toxoplasma gondii* infection (11).

Since MyD88 is a critical component in the signaling cascade mediated by the IL-1 receptor and TLR, as well as the IL-18 receptor, it is thought that MyD88 plays a key role in mycobacterial infection. The present study was undertaken to determine the role of MyD88 in murine tuberculosis *in vivo*. Although MyD88 plays an important role in the host defense against mycobacterial infection, the results in this study suggest that there may be a TLR2-specific MyD88-independent signaling pathway which activates NF-κB in mycobacterial infection.

**Address correspondence to* Dr. Isamu Sugawara, Mycobacterial Reference Center, The Research Institute of Tuberculosis, 3–1–24 Matsuyama, Kiyose, Tokyo 204–0022, Japan. Fax: 81–424–92–4600. E-mail: sugawara@jata.or.jp

Materials and Methods

Animals. Six-week-old C57BL/6 wild-type (WT) mice were purchased from Japan SLC Co., Ltd. (Shizuoka, Japan), and C57BL/6 MyD88 knockout (KO) mice were supplied from the Research Institute for Microbial Diseases, Osaka University (19). These KO mice showed no developmental abnormalities. All mice were housed in a biosafety level 3 facility and given mouse chow and water *ad libitum* after aerosol infection with virulent mycobacteria.

Experimental infections. A virulent Kurono strain of *Mycobacterium tuberculosis* (ATCC 358121) was grown in Middlebrook 7H9 broth for 2 weeks, then filtered with a sterile acrodisc syringe filter (Pall Corp., Ann Arbor, Mich., U.S.A.) with a pore size of 5.0 μm. Then, the aliquots of the filtrate bacterial solution were stored at −80 C until use. Mice were infected via the airborne route by placing them in the exposure chamber of the Glas-Col aerosol generator (Glas-Col, Inc., Terre

Abbreviations: CFU, colony-forming unit; KO, knockout; TLR, *Toll*-like receptor; WT, wild-type.

Haute, Ind., U.S.A.). The nebulizer compartment was filled with 5 ml of a suspension containing 10^6 CFU of Kurono tubercle bacilli so that approximately 100 bacteria might be deposited in the lungs of each animal (13, 24). Inhalation infection experiments were carried out twice. Several infected mice were monitored for up to 6 months for survival.

CFU assay. At 1, 3, 5, 7, and 12 weeks after aerial infection, mice were anesthetized with pentobarbital sodium. The abdominal cavity was incised, and exsanguination was done by splenectomy. Lungs, spleens, and livers were excised and weighed. The left lobe of each lung and a part of spleen tissue separately were weighed and used to evaluate *in vivo* growth of mycobacteria. The lung and spleen tissues were homogenized with a set of mortar and pestle, and 1 ml of sterile saline was added. Then, 100 μl of homogenate was picked up and plated in a 10-fold serial dilution on 1% Ogawa's egg media. Colonies on the media were counted after a 4-week incubation at 37 C (24).

RT-PCR. Parts of the right lobe of the lung and spleen tissues that had been left after cutting off for CFU examination were used to perform RT-PCR analysis for mRNA expression for several cytokines and iNOS in these organs during *M. tuberculosis* infection. These tissue samples were snap-frozen in liquid nitrogen and stored at −85 C until use. RNA extraction was performed as previously described (15, 24). Briefly, frozen tissues were homogenized with a microcentrifuge tube and tip-closed 1 ml pipet tip in liquid nitrogen. Then, homogenates were treated with a total RNA isolation reagent, TRIzol™ Reagent (GIBCO BRL), according to a manufacturer's instructions. After RNA isolation, total RNA was reverse transcribed into cDNA with M-MLV reverse transcriptase (GIBCO BRL) following measurement of total RNA concentration, and agarose gel electrophoresis was performed.

Polymerase chain reaction was performed with gene-specific primer sets for β-actin, IFN-α, IFN-β, IFN-γ, TNF-α, interleukin (IL)-1β, IL-2, IL-4, IL-6, IL-10, IL-12p40, IL-18, TGF-β, and iNOS. DNA sequences of primer sets and corresponding PCR conditions are summarized as previously described (17). The PCR primer sets for ICAM-1 mRNA are as follows: sense, 5'-TGCGTTTTGGAGCTAGCGGACCA-3'; antisense, 5'-CGAGGACCATACAGCACGTGCAG-3'. The expected product length is 326 bp. Amplification was carried out with a DNA thermal cycler 480 (Perkin-Elmer Cetus). PCR product (10 μl each) was applied for electrophoresis in 4% agarose and NuSieve GTG (1:3) gel and visualized using ethidium bromide staining. Relative amplification ratios of various cytokines and iNOS mRNA to β-actin mRNA as an internal control were determined (16).

Light microscopic examination. For light microscopic examination, the right middle lobe of each lung was excised and fixed with 20% formalin buffered methanol solution, Mildform 20NM (containing 8% formaldehyde and 20% methanol, Wako Pure Chemical Co., Osaka, Japan), then dehydrated with grading series of ethanol, treated with xylene, and embedded in paraffin. The 5 mm-thick sections were cut from each paraffin block and stained with either hematoxylin and eosin or Ziehl-Neelsen staining. We prepared every lung tissue with gray nodular lesions. The sizes of the 10 granulomas were measured with a micrometer (Nikon Optical Co., Tokyo) (13).

Cytokine assays. Murine blood were prepared by cardiac puncture of MyD88 KO and WT mice 3 weeks after aerosol infection with *M. tuberculosis* Kurono strain. The blood was coagulated at 4 C and centrifuged at 2,000 rpm for 20 min to obtain sera. The concentrations of IFN-γ, TNF-α, IL-1β, and IL-12 in the sera were measured in triplicate by sandwich enzyme-linked immunosorbent assay (ELISA) (Biosource International, Inc., Calif., U.S.A.) (13).

Electrophoretic mobility shift assay for NF-κB activity. The alveolar macrophages were obtained from the lung tissues of MyD88-deficient and WT mice by bronchoalveolar lavage (BAL). These alveolar macrophages were cultured with H37Rv (m. o. i.; 10:1) overnight at 37 C in a CO_2 incubator. The collected alveolar macrophages were treated in 5 ml of solution A (0.6% NP40, 150 mM NaCl, 10 mM HEPES, pH 7.9, 1 mM EDTA, and 0.5 mM phenylmethylsulfonyl fluoride). The supernatant containing the DNA-binding proteins was divided into small fractions, frozen in liquid nitrogen, and stored at −80 C (5). EMSA using NF-κB probes (Promega) was performed as previously described (18, 20). The specificity of binding was determined by competition with the unlabeled oligonucleotide.

Statistical methods. The values were compared by Student's *t* test. The level of significance was calculated between groups and by nonparametric equivalents of analysis of variance for multiple comparison (18).

Results

Mycobacterial Burden in the Lungs and Spleens of MyD88 KO Mice

The mycobacterial load in the infected lungs and spleens of MyD88 knockout (KO) mice was evaluated. The KO and wild-type (WT) mice were infected by placing them into the exposure chamber of an aerosol generator (Glas-Col, Inc.) in which the nebulizer compartment was filled with 5 ml of a suspension containing

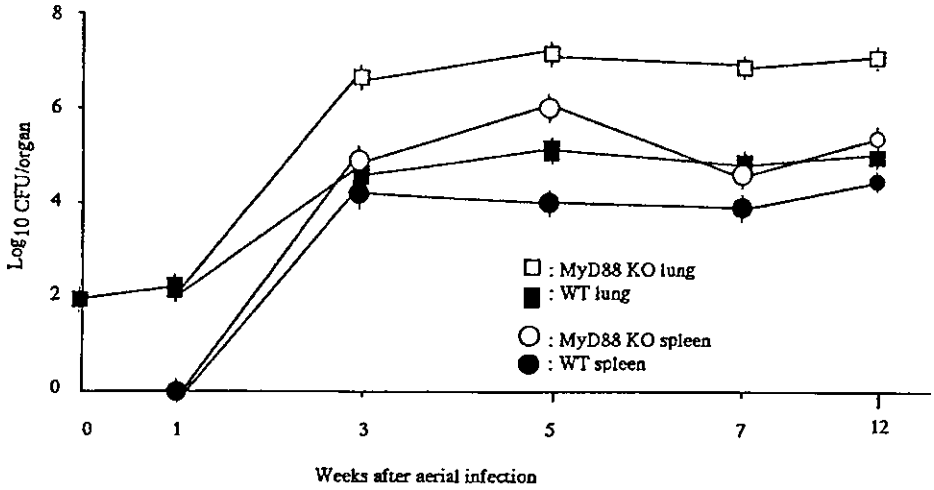

Fig. 1. Colony-forming units (CFU) in the lungs and spleen tissues of MyD88 KO and WT mice (12 mice each) exposed to 10^6 CFU of *M. tuberculosis* Kurono strain by the airborne route. At the time indicated (weeks after infection), three mice from each group were sacrificed and homogenates of the lungs and spleens were plated. Error bars indicate standard deviation (SD) from the mean.

10^6 colony-forming units (CFU) of Kurono strain tubercle bacilli under conditions that introduced approximately 100 tubercle bacilli into the lungs of each animal. Both MyD88 KO and age- and sex-matched C57BL/6 WT mice survived the entire 12-week experimental period. When several infected MyD88 KO mice were monitored for 6 months, they did not die. The numbers of tubercle bacilli recovered from the lungs and spleens of infected animals after aerosol infection are shown as CFU in Fig. 1. One week after infection, tubercle bacilli were recovered only from the lung tissues of MyD88 KO and WT mice. However, 5 weeks after infection, the mycobacterial load in the lungs had increased in MyD88 KO mice. There was a statistically significant difference in pulmonary CFU between MyD88 KO and WT mice ($P<0.01$). Seven weeks after infection, the bacterial load gradually decreased. Both the MyD88 KO and WT mice showed similar patterns of bacterial growth in the spleen tissues. There was a statistically significant difference in spleen CFU at 5 weeks after infection between MyD88 KO and WT mice ($P<0.01$). On the other hand, in WT mice, the bacterial load in the lungs and spleens reached a peak at 5 weeks and 3 weeks after infection, respectively.

Light Microscopic Observation of Infected Lungs

Histopathological findings obtained from MyD88 KO and WT mice showed similar granulomatous lesions after infection. Figure 2A shows a large discrete pulmonary granuloma with neutrophil infiltration, which was compared with the lesions observed in WT mice (Fig. 2C). A relatively large number of tubercle bacilli were recognized in the granulomatous lesion (Fig. 2B). No neutrophil infiltration was observed in the pulmonary granulomas of WT mice. The average diameter of 10 granulomas in the lungs of MyD88 KO mice was 9,860±90 μm, whereas that of WT mice was 5,050±45 μm ($P<0.01$).

RT-PCR Analysis

Because the mycobacterial CFU assay and histopathological examination indicated that MyD88 KO mice were more susceptible to *Mycobacterium tuberculosis* than WT mice, RT-PCR was carried out to compare the expression levels of mRNAs for the major cytokines, TGF-β, ICAM-1, and iNOS in the lung tissues of MyD88 KO and WT mice. Figure 3 shows the results of RT-PCR with infected lung tissues 1, 3, 5, 7, and 12 weeks after infection. Expression of IL-18 and iNOS mRNA in MyD88 KO mice was slightly lower than that in WT mice until 12 weeks after infection. Expressions of TNF-α, IL-12, and ICAM-1 mRNA were similar in both MyD88 KO and WT mice. On the other hand, expressions of IFN-γ, IL-1β, IL-2, IL-4, IL-6, IL-10, and TGF-β mRNA were significantly higher in MyD88 KO mice than in WT mice.

Cytokine Assay

We examined the *in vivo* cytokine secretion capacity in sera from MyD88 KO mice 3 weeks after aerosol infection. As shown in Table 1, concentrations of IFN-α, TNF-α, IL-1β, and IL-12 were high in the sera of MyD88 KO mice. Compared with those of WT mice, there was no statistically significant difference in the cytokine secretion capability.

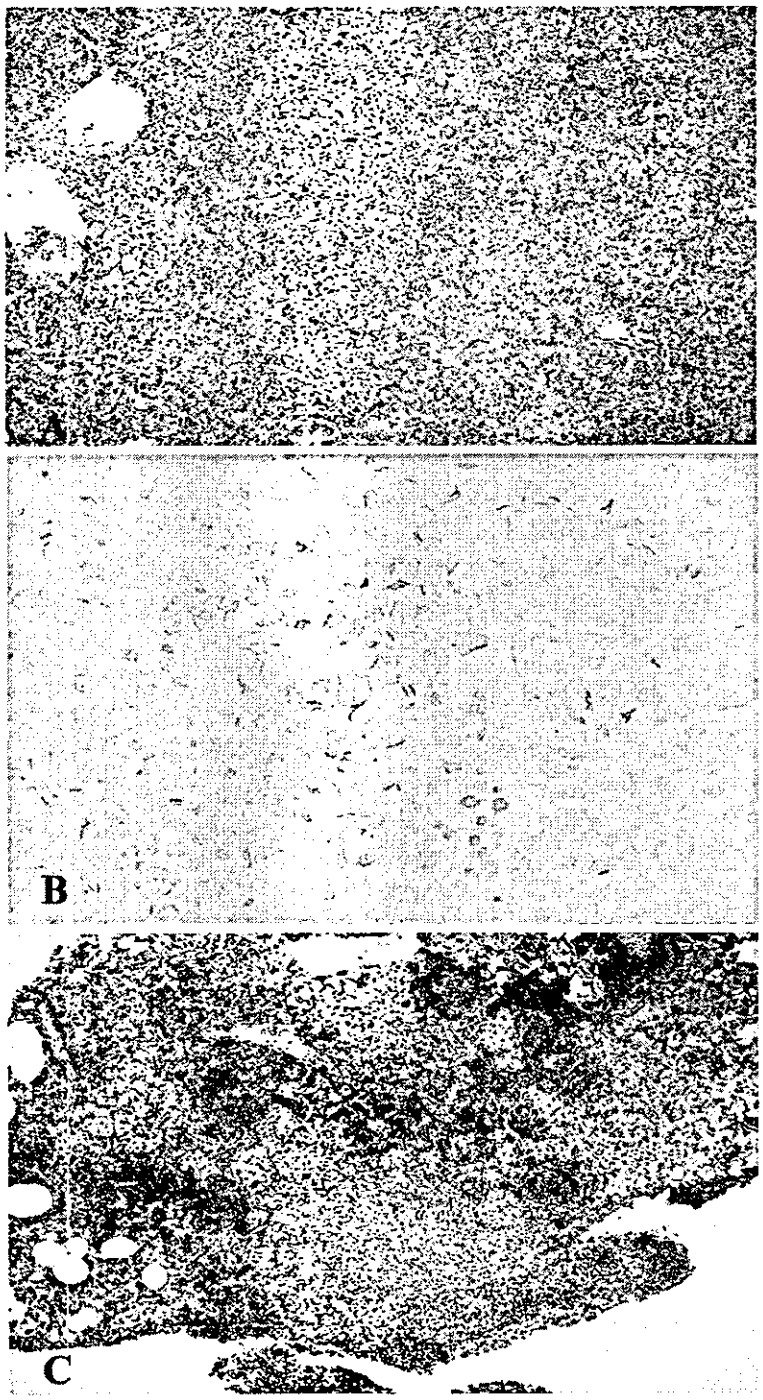

Fig. 2. Histopathologic examination of infected lung tissue. Mice were sacrificed 5 weeks after infection, and formalin-fixed sections were stained with hematoxylin and eosin (A and C) and Ziehl-Neelsen stain for acid-fast bacilli (B). (A) Pulmonary tissue from an MyD88 KO mouse infected with the Kurono strain. A large granulomatous lesion with neutrophil infiltration can be observed. Magnification, ×100. (B) Pulmonary tissue from an MyD88 KO mouse infected with the Kurono strain. Many acid-fast bacilli can be seen in the granulomatous lesion by Ziehl-Neelsen staining. Magnification, ×600. (C) Pulmonary tissue from a WT mouse infected with the Kurono strain. A discrete granuloma can be observed. Magnification, ×100.

Electrophoretic Mobility Shift Assay

An electrophoretic mobility shift assay (EMSA) was carried out to measure NF-κB activity in the H37Rv-treated and untreated alveolar macrophages from the MyD88 KO and WT mice. As shown in Fig. 4, NF-κB activity in MyD88 KO mice was slightly lower than in WT mice. Contrary to our expectation that NF-κB activity was reduced in *M. tuberculosis*-infected MyD88 KO mice, significant NF-κB activity was observed even in the absence of MyD88.

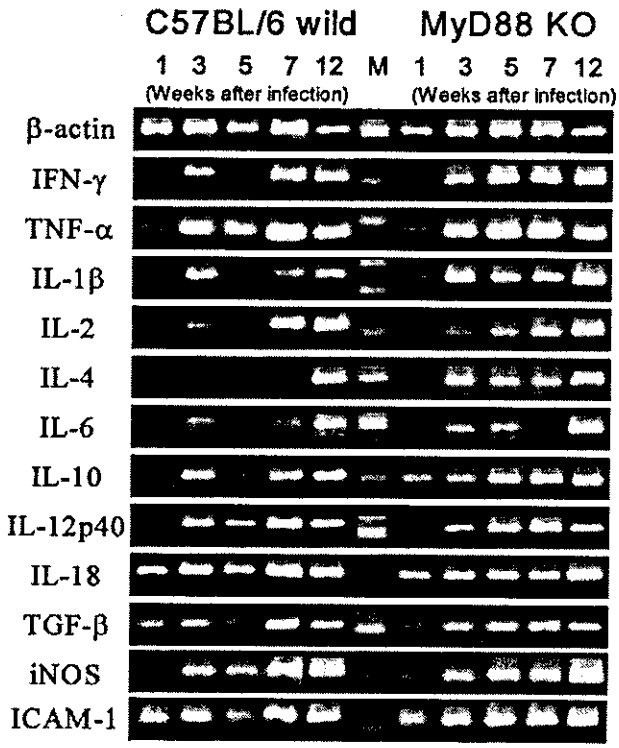

Fig. 3. *In vivo* expressions of mRNAs for various cytokines and iNOS in Kurono strain-infected mice by RT-PCR. Lung tissue of MyD88 KO and WT mice (three mice/time point) were removed 1, 3, 5, 7, and 12 weeks after airborne infection. Inhalation infection experiments were performed twice. β-Actin gene primer sets were used as internal controls. M, size marker.

Discussion

We have found that large granulomas were induced by aerial infection of an *M. tuberculosis* strain but that necrotic lesions were not recognized in major organs including lungs, spleens, livers, hilar lymph nodes, and kidneys. This finding is interesting because it has been reported that MyD88-deficient mice are highly susceptible to *Staphylococcus aureus* infection (19). This discrepancy is explained as follows. *Staphylococcus aureus* infection is acute and *M. tuberculosis* infection is chronic. MyD88 may play a major role in defense against acute infection. Even in the absence of MyD88, the TNF-α/TNF-α receptor-mediated signaling pathway

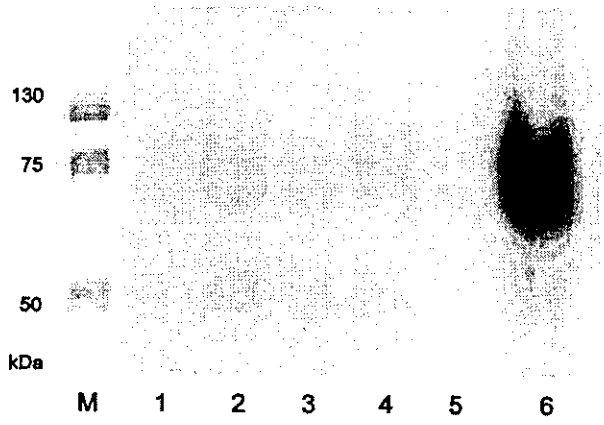

Fig. 4. NF-κB activity in alveolar macrophages infected with H37Rv overnight. Lane M, size marker; lane 1, alveolar macrophages from WT mice; lane 2, alveolar macrophages after *in vitro* infection with H37Rv from WT mice; lane 3, alveolar macrophages from MyD88 KO mice; lane 4, alveolar macrophages after *in vitro* infection with H37Rv from MyD88 KO mice; lane 5, competition of the nuclear protein in alveolar macrophages from WT mice after overnight *in vitro* infection with H37Rv with the unlabeled oligonucleotides; and lane 6, alveolar macrophages from WT mice treated with LPS (10 μg/ml). Similar experiments were carried out twice. The upper band shows p65 and the lower band shows p50. NF-κB activity is similar in MyD88 KO and WT mice.

Table 1. Cytokine secretion in sera of *M. tuberculosis*-infected MyD88 KO mice

Mouse	Amount (pg/ml) of cytokine in sera of mice 3 weeks after aerosol Infection[a]			
	IFN-γ	TNF-α	IL-1β	IL-12
MyD88 KO	500±10	4,000± 50	750±50	350±10
WT	550±50	4,300±100	600±50	400±20

[a] Values are means±standard error (SE) of the means of two independent experiments. No significant difference was found in the cytokine secretion between MyD88 KO and WT mice.

operates in mycobacterial infection to activate NF-κB that regulates expressions of IL-1, IL-2, IL-6, TNF-α, IFN-γ, and ICAM-1 mRNA (8). More importantly, this TNF-α/TNF-α receptor-mediated signaling pathway does not require MyD88 as an adaptor molecule. Of course, this does not rule out the possibility that there may be a TLR2-specific MyD88-independent IL-1/TLR-mediated NF-κB activation pathway, although its presence has not yet been confirmed. Akira et al. reported that activation of NF-κB is induced in response to lipopolysaccharides (LPS) despite the absence of MyD88 (2). The TLR4 signal has a TLR4-specific MyD88-independent pathway that is involved in induction of type I interferons and IFN-inducible genes via IFN regulatory factor-3 activation. They even suggest the presence of *Toll*-IL receptor domain-containing adaptor protein in the TLR4-specific MyD88-independent pathway. Our results suggest that there is a TLR2-specific MyD88-independent NF-κB activation pathway although its function remain unknown.

We have shown that NK-κB plays a critical role in the defense against mycobacterial infection (24). Contrary to our expectations that NF-κB activity is reduced in MyD88 KO mice because MyD88-deficient mice developed large granulomatous pulmonary lesions, significant NF-κB activity was observed in MyD88-deficient mice. There may be two possible explanations for this. One is the presence of a TNF-α/TNF-α receptor-mediated NF-κB activation pathway in which MyD88 is not required as an adaptor protein. As TNF-α mRNA is induced at the same level in MyD88 KO mice as in WT mice, NF-κB activity is induced as usual in our present experiments. In the absence of TNF-α, *M. tuberculosis*-infected mice die due to multiple disseminated necrotic lesions with numerous tubercle bacilli (9). The other explanation is that there may be a TLR2-specific MyD88-independent IL-1/TLR-mediated NF-κB activation pathway, although its presence has not yet been clarified. Although Akira et al. suggest that the TLR4 signal has a TLR4-specific MyD88-independent pathway, he does not mention whether or not the TLR2 signal has a TLR2-specific MyD88-independent pathway (2). Under this condition, NF-κB activity is not reduced in MyD88 KO mice.

MyD88-deficient mice developed more advanced pulmonary lesions than WT mice in terms of CFU and histopathology. However, expression levels of IL-12, TNF-α, and IFN-γ mRNA in MyD88-deficient mice are not different from those of WT mice. A similar tendency also was observed in the sera obtained from MyD88 KO and WT mice infected with *M. tuberculosis* Kurono strain for 3 weeks. As already reported, these are important factors in the defense against mycobacerial infection (3, 4, 6, 7, 9, 12). Transcription factors including NF-κB, NF-IL6, IRF-1, and STAT4 also are important in the defense against mycobacterial infection (15–17, 24, 25). This may indicate the presence of yet unknown cytokine(s) and transcription factor(s) contributing to progression of tuberculosis because there exists a discrepancy between large pulmonary granulomas and normal expression of IL-12, TNF-α, and IFN-γ mRNA in MyD88 KO mice. Low expressions of IL-1, IL-2, IL-6, TNF-α, IFN-γ, and ICAM-1 mRNA in MyD88 KO mice are expected because it is thought that these cytokines are regulated by NF-κB, which is low in the absence of MyD88 (8). At present, we cannot explain why IFN-γ, IL-1β, IL-2, IL-4, IL-6, IL-10, and TGF-β mRNA were expressed at higher levels in MyD88 KO mice than in WT mice. Further studies are required to clarify this.

In summary, there may be a TLR2-specific MyD88-independent IL-1 receptor/TLR-mediated NF-κB activation pathway and that MyD88 deficiency does not affect the development of murine tuberculosis although MyD88 itself plays an important role in the TLR-mediated NF-κB activation pathway.

This study was supported in part by an International Collaborative Study Grant to the chief investigator, Dr. Isamu Sugawara, from the Ministry of Health, Labour and Welfare, Japan. The authors would like to acknowledge Dr. Masashi Desaki, University of Tokyo Faculty of Medicine, for his help with the EMSA assay for NF-κB.

References

1) Adachi, O., Kawai, T., Takeda, K., Matsumoto, M., Tsutsui, H., Sakagami, M., Nakanishi, K., and Akira, S. 1998. Targeted disruption of the MyD88 gene results in loss of IL-1 and IL-18-mediated function. Immunity **9**: 143–150.
2) Akira, S., and Hoshino, K. 2003. Myeloid differentiation factor 88-dependent and -independent pathways in Toll-like receptor signaling. J. Infect. Dis. **187** (Suppl 2): 356–363.
3) Cooper, A.M.D., Dalton, D.K., Stewart, T.A., Griffin, J.P., Russell, D.G., and Orme, I.M. 1993. Disseminated tuberculosis in interferon-γ gene-disrupted mice. J. Exp. Med. **178**: 2243–2247.
4) Cooper, A.M., Magram, J., Ferrante, J., and Orme, I.M. 1997. IL-12 is critical to the development of protective immunity in mice intravenously infected with *Mycobacterium tuberculosis*. J. Exp. Med. **186**: 39–45.
5) Deryckere, F. and Cannon, F. 1994. A one-hour minipreparation technique for extraction of DNA-binding proteins from animal tissues. Biotechniques **16**: 405.
6) Flynn, J.L., Chan, J., Triebold, K.J., Dalton, T.K., Stewart, T.A., and Bloom, B.R. 1993. An essential role for interferon-γ in resistance to *Mycobacterium tuberculosis* infection. J. Exp. Med. **178**: 2249–2254.
7) Flynn, J.L., Goldstein, M.M., Chan, J., Triebold, K.J., Pfeffer, K., Lowenstein, C.J., Schreiber, R., Mak, T., and Bloom,

B.R. 1995. Tumor necrosis factor-α is required in the protective immune response against *Mycobacterium tuberculosis* in mice. Immunity **2**: 561–572.
8) Ghosh, S., May, M.J., and Kopp, E.B. 1998. NF-κB and Rel proteins: evolutionary conserved mediators of immune responses. Ann. Rev. Immunol. **16**: 225–260.
9) Kaneko, H., Yamada, H., Kazumi, Y., Mizuno, S., Sekikawa, K., and Sugawara, I. 1999. Role of tumor necrosis factor-α in *Mycobacterium*-induced granuloma formation in tumor necrosis factor-α-deficient mice. Lab. Invest. **79**: 379–386.
10) Kawai, T., Adachi, O., Ogawa, T., Takeda, K., and Akira, S. 1999. Unresponsiveness of MyD88-deficient mice to endotoxin. Immunity **11**: 115–122.
11) Scanga, C.A., Aliberti, J., Jankovic, D., Tilloy, F., Bennouna, S., Denkers, E.Y., Medzhitov, R., and Sher, A. 2002. Cutting edge: MyD88 is required for resistance to *Toxoplasma gondii* infection and regulates parasite-induced IL-12 production by dendritic cells. J. Immunol. **168**: 5997–6001.
12) Sugawara, I., Yamada, H., Otomo, K., Aoki, T., Doi, N., Kazumi, Y., Tagawa, Y., and Iwakura, Y. 1998. Induction of granulomas in interferon-γ gene-disrupted mice by avirulent but not by virulent strains of *Mycobacterium tuberculosis*. J. Med. Microbiol. **47**: 871–877.
13) Sugawara, I., Yamada, H., Kaneko, H., Mizuno, S., Takeda, K., and Akira, S. 1999. Role of IL-18 in mycobacterial infection in IL-18-gene-disrupted mice. Infect. Immun. **67**: 2585–2589.
14) Sugawara, I., Yamada, H., Hua, S., and Mizuno, S. 2001. Role of IL-1 type 1 receptor in mycobacterial infection. Microbiol. Immunol. **45**: 743–750.
15) Sugawara, I., Mizuno, S., Yamada, H., Matsumoto, M., and Akira, S. 2001. Disruption of nuclear factor-IL-6, a transcription factor, results in severe mycobacterial infection. Am. J. Pathol. **158**: 361–366.
16) Sugawara, I., Yamada, H., Mizuno, S., Li, C., Nakayama, T., and Taniguchi, M. 2002. Mycobacterial infection in natural killer T cell knockout mice. Tuberculosis **82**: 97–104.
17) Sugawara, I., Yamada, H., and Mizuno, S. 2003. Relative importance of STAT 4 in murine tuberculosis. J. Med. Microbiol. **52**: 29–34.
18) Sugawara, I., Yamada, H., Li, C., Mizuno, S., Takeuchi, O., and Akira, S. 2003. Mycobacterial infection in TLR2 and TLR6 knockout mice. Microbiol. Immunol. **47**: 327–336.
19) Takeuchi, O., Hoshino, K., and Akira, S. 2000. Cutting edge: TLR2-deficient and MyD88-deficient mice are highly susceptible to *Staphylococcus aureus* infection. J. Immunol. **165**: 5392–5396.
20) Takizawa, H., Ohtoshi, T., Kawasaki, S., Kohyama, T., Desaki, M., Kasama, T., Kobayashi, K., Nakahara, K., Yamamoto, K., Matsushima, K., and Kudoh, S. 1999. Diesel exhaust particles induce NF-κB activation in human bronchial epithelial cells *in vitro*: importance in cytokine transcription. J. Immunol. **162**: 4705–4711.
21) Thoma-Uszynski, S., Stenger, S., Takeuchi, O., Ochoa, M.T., Engele, M., Sieling, P.A., Barnes, P.F., Rollinghoff, M., Bolcskei, P.L., Wagner, M., Akira, S., Norgard, M.V., Belisle, J.T., Godowski, P.J., Bloom, B.R., and Modlin, R.L. 2000. Induction of direct antimicrobial activity through mammalian Toll-like receptors. Science **291**: 1544–1547.
22) Underhill, D.M., Ozinsky, A., Smith, K.D., and Aderem, A. 1999. Toll-like receptor-2 mediates mycobacteria-induced proinflammatory signaling in macrophages. Proc. Natl. Acad. Sci. U.S.A. **96**: 14459–14463.
23) Yamada, H., Mizuno, S., Horai, R., Iwakura, Y., and Sugawara, I. 2000. Protective role of IL-1 in mycobacterial infection in IL-1α/β double-knockout mice. Lab. Invest. **80**: 759–767.
24) Yamada, H., Mizuno, S., Reza-Gholizadeh, M., and Sugawara, I. 2001. Relative importance of NF-κB p50 in mycobacterial infection. Infect. Immun. **69**: 7100–7105.
25) Yamada, H., Mizuno, S., and Sugawara, I. 2002. Interferon regulatory factor 1 in mycobacterial infection. Microbiol. Immunol. **46**: 751–760.

Microbiol. Immunol., 47(5), 327–336, 2003

Mycobacterial Infection in TLR2 and TLR6 Knockout Mice

Isamu Sugawara*[,1], Hiroyuki Yamada[1], Chuanyou Li[1], Satoru Mizuno[1], Osamu Takeuchi[2], and Shizuo Akira[2]

[1]*Department of Molecular Pathology, The Research Institute of Tuberculosis, Kiyose, Tokyo 204–0022, Japan, and* [2]*Department of Host Defense, Research Institute for Microbial Diseases, Osaka University, Suita, Osaka 565–0871, Japan*

Received January 9, 2003. Accepted February 13, 2003

Abstract: **To investigate the role of TLR in the development of murine tuberculosis *in vivo*, TLR2 and TLR6 knockout (KO) mice were infected with *Mycobacterium tuberculosis* by placing them in the exposure chamber of an airborne infection apparatus. Both TLR2 and TLR6 KO mice survived until sacrifice at 12 weeks after infection. Infected TLR2 KO mice developed granulomatous pulmonary lesions with neutrophil infiltration, which were slightly larger in size than those in wild-type mice. Pulmonary levels of the mRNAs for inducible nitric oxide synthase (iNOS), TNF-α, TGF-β, IL-1β, and IL-2 were significantly lower, but levels of the mRNAs for IL-4 and IL-6 were higher, than in wild-type (WT) mice. No significant difference was recognized in cytokine mRNA expression between TLR2 KO and WT mice at 12 weeks after infection. DNA binding by NF-κB was low in TLR2 KO mice. On the other hand, TLR6 KO mice were not different from WT mice in terms of pulmonary histopathology, mRNA expression and CFU assay. Therefore, TLR2 does not play an essential role in the pathogenesis of murine tuberculosis, although it is important for defense against mycobacterial infection.**

Key words: ***Mycobacterium tuberculosis*, TLR2, TLR2 knockout mouse, TLR6, NF-κB**

Toll-like receptor (TLR) family members are differentially expressed among many immune cells and respond to different stimuli (2–4). The TLR family includes TLR2, TLR4, TLR5, TLR6 and TLR9. TLR2 recognizes a variety of microbial products. Cell activation induced by *Mycoplasma fermentans* lipoprotein is mediated by TLR2 (19). TLR2 plays a major role in recognition of Gram-positive bacteria, but TLR4 is essential for signaling via LPS from Gram-negative bacteria (25). TLR4 recognizes endogenous host-derived products as well as viral and plant products. Recognition by TLR5 and TLR9 is much more restricted, and essential for flagellin- and CpG DNA-mediated signaling, respectively, compared with TLR2 and TLR4 (13, 14).

Viable *M. tuberculosis* bacilli contain distinct ligands that activate cells via the mammalian TLR proteins TLR2 and TLR4 *in vitro* (18). In fact, 19 kDa lipoprotein and lipoarabinomannan from rapidly growing mycobacteria bind to TLR2 (6, 17, 20). Several *in vitro* studies have suggested active participation of TLR2 in mycobacterial inflammation (6, 27, 28). It has been shown that activation of TLR2 leads to killing of intracellular *M. tuberculosis* in both mouse and human macrophages (27). Viable *M. tuberculosis* bacilli activate both Chinese hamster ovary cells and murine macrophages overexpressing either TLR2 or TLR4 (17). Bulut et al. have suggested a functional interaction between TLR2 and TLR6 in the cellular response to soluble tuberculosis factor and *Borrelia burgdorferi* outer surface protein A lipoprotein (7). Thus, it is unclear whether TLR2 alone is involved in the response to *M. tuberculosis* infection, or whether TLR2 and TLR4, or TLR2 and TLR6, act together.

The present study was undertaken to clarify the roles of TLR2 and TLR6 in mycobacterial infection *in vivo*. We used TLR2 and TLR6 KO mice (25) in a model of pulmonary infection with Kurono strain, and showed that TLR2 is important for the development of protective immunity, although these infected mice did not develop the acute disseminated form of mycobacterial infection.

**Address correspondence to* Dr. I. Sugawara, Department of Molecular Pathology, The Research Institute of Tuberculosis, 3-1-24 Matsuyama, Kiyose, Tokyo 204–0022, Japan. Fax: 81–424–92–4600. E-mail: sugawara@jata.or.jp

Abbreviations: CFU, colony-forming unit; KO, knockout; TLR, *Toll*-like receptor; WT, wild-type.

Materials and Methods

Mice. Six-week-old C57BL/6 wild-type mice were purchased from Japan SLC, Co., Ltd. (Shizuoka, Japan). TLR2 and TLR6 KO mice of C57BL/6 origin were generated as described previously (25). The TLR2 and TLR6 KO mice did not show any developmental abnormalities. All mice were housed in a biosafety level 3 facility and given mouse chow and water *ad libitum* after aerosol infection with mycobacteria.

Experimental infections. The virulent Kurono strain of *Mycobacterium tuberculosis* (ATCC 358121) was grown in Middlebrook 7H9 broth for 2 weeks, then filtered with a sterile acrodisc syringe filter (Pall Corporation, Ann Arbor, Mich., U.S.A.) with a pore size of 5.0 μm. Aliquots of the filtered bacterial suspension were stored in a freezer at −80 C until use. The mice were infected by placing them into the exposure chamber of an aerosol generator (Glas-Col, Inc., Terre Haute, Ind., U.S.A.) in which the nebulizer compartment was filled with 5 ml of a suspension containing 10^6 CFU of Kurono tubercle bacilli under conditions that would introduce about 100 bacteria into the lungs of each animal (23, 30).

CFU assay. At 1, 3, 5, 7, and 12 weeks after aerosol infection, groups of mice were anesthetized with pentobarbital sodium, the abdominal cavities were incised, and exsanguination was carried out by splenectomy and transection of the left renal artery and vein. The lung and spleen tissue samples were homogenized with a mortar and pestle, then placed in test tubes, and 1 ml of sterile saline was added to each sample. After homogenization, 100 μl of the homogenate was plated in 10-fold serial dilution on 1% Ogawa slant media. Colonies on the media were counted after a 4-week incubation at 37 C (30).

Reverse transcriptase (RT)-polymerase chain reaction (PCR). The right lobes of the lungs and the spleen tissues were used for RT-PCR analysis to examine expression levels of the mRNAs for several cytokines during *M. tuberculosis* infection. The tissue samples were snap-frozen in liquid nitrogen and stored at −85 C until use. RNA extraction was performed as described previously (29, 30). Briefly, the frozen tissues were homogenized in a microcentrifuge tube. Then the homogenates were treated with the total RNA isolation reagent TRIzol (GIBCO BRL) according to the manufacturer's instructions. After RNA isolation, total RNA was reverse-transcribed into cDNA with M-MLV reverse transcriptase (GIBCO BRL) following measurement of total RNA concentration, and agarose gel electrophoresis was performed.

PCR was performed with gene-specific primer sets for the β-actin, IFN-α, IFN-β, IFN-γ, TNF-α, interleukin (IL)-1β, IL-2, IL-6, IL-10, IL-12p40, IL-18, TGF-β, and iNOS genes. For β-actin, samples were subjected to 23 cycles of denaturation (94 C for 1 min), annealing (65 C for 1 min), and extension (72 C for 2 min); for IFN-α, IFN-γ, TNF-α, IL-1β, IL-12p40 and iNOS, 30 cycles of denaturation (94 C for 1 min), annealing (65 C for 1 min), and extension (72 C for 2 min); for IL-2 and IL-6, 40 cycles of denaturation (94 C for 1 min), annealing (62 C for 1 min), and extension (72 C for 2 min); for IL-10, 40 cycles of denaturation (94 C for 1 min), annealing (65 C for 1 min), and extension (72 C for 2 min); for TGF-β, 25 cycles of denaturation (94 C for 1 min), annealing (60 C for 1 min), and extension (72 C for 2 min); for IFN-β, 33 cycles of denaturation (94 C for 1 min), annealing (65 C for 1 min), and extension (72 C for 1 min); for IL-18, denaturation (94 C for 1 min), annealing (58 C for 1 min) and extension (72 C for 1 min).

The primer sequences and PCR product sizes were as follows: for β-actin, 5′-TGT GAT GGT GGG AAT GGG TCA G-3′ (sense) and 5′-TTT GAT GTC ACG CAC GAT TTC C-3′ (antisense), 514 bp; for IFN-γ, 5′-TAC TGC CAC GGC ACA GTC ATT GAA-3′ (sense) and 5′-GCA GCG ACT CCT TTT CCG CTT CCT-3′ (antisense), 405 bp; for TNF-α, 5′-ATG AGC ACA GAA AGC ATG ATC-3′ (sense) and 5′-TAC AGG CTT GTC ACT CGA ATT-3′, 276 bp; for IL-1β, 5′-CAG GAT GAG GAC ATG AGC ACC-3′ (sense) and 5′-CTC TGC AGA CTC AAA CTC CAC-3′ (antisense), 447 bp; for IL-2, 5′-CTT CAA GCT CCA CTT CAA GCT-3′ (sense) and 5′-CCA TCT CCT CAG AAA GTC CAC-3′ (antisense), 400 bp; for IL-6, 5′-CAT CCA GTT GCC TTC TTG GGA-3′ (sense) and 3′-CAT TGG GAA ATT GGG GTA GGA AG-3′ (antisense), 463 bp; for IL-10, 5′-CCA GTT TTA CCT GGT AGA AGT GAT-3′ (sense) and 5′-TGT CTA GGT CCT GGA GTC CAG CAG-3′ (antisense), 324 bp; for IL-12p40, 5′-ATC TCC TGG TTT GCC ATC GTT TTG-3′ (sense) and 5′-TCC CTT TGG TCC AGT GTG ACC TTC-3′ (antisense), 527 bp; for TGF-β, 5′-CGG GGC GAC CTG GGC ACC ATC CAT GAC-3′ (sense) and 5′-CTG CTC CAC CTT GGG CTT GCG ACC CAC-3′ (antisense), 371 bp; for iNOS, 5′-TGG GAA TGG AGA CTG TCC CAG-3′ (sense) and 5′-GGG ATC TGA ATG TGA TGT TTG-3′ (antisense), 306 bp.

Amplification was carried out with a thermal cycler (model 480, Perkin-Elmer Cetus). Each PCR product (10 μl) was subjected to electrophoresis in 4% agarose and NuSieve GTG (1:3) gel and visualized by ethidium bromide staining (24, 30).

Light and electron microscopy. For light microscopy, the left lobes of the lungs were excised and fixed with 20% formalin-buffered methanol solution, Mildform

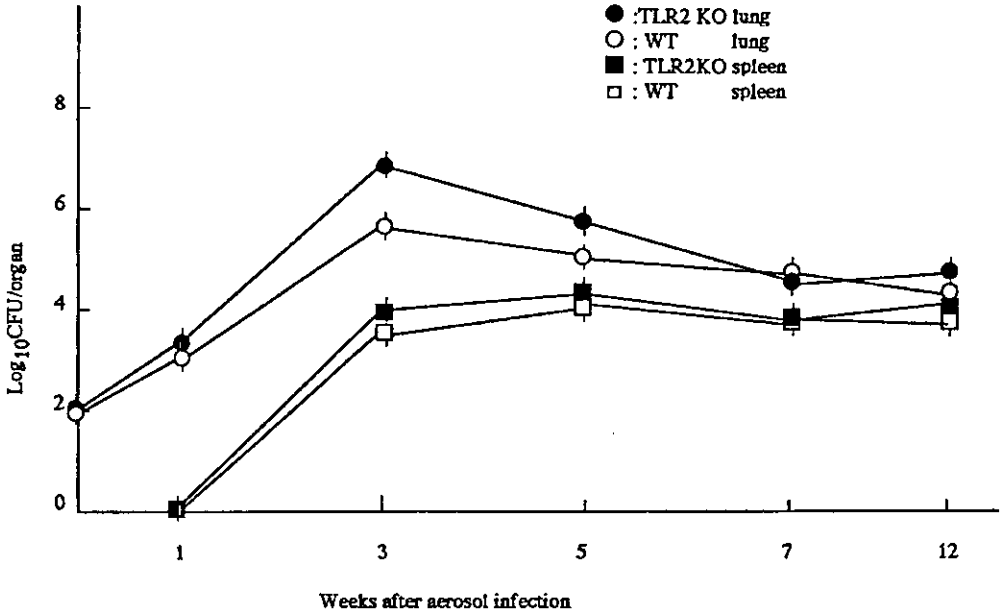

Fig. 1. CFU in lung and spleen tissues of TLR2 KO and WT mice (12 mice each) exposed to 10^6 CFU of *M. tuberculosis* Kurono strain by the airborne route. At the indicated weeks after infection, three mice from each group were sacrificed and homogenates of the lung and spleen tissues were plated. Error bars indicate standard deviations (SD) of the means.

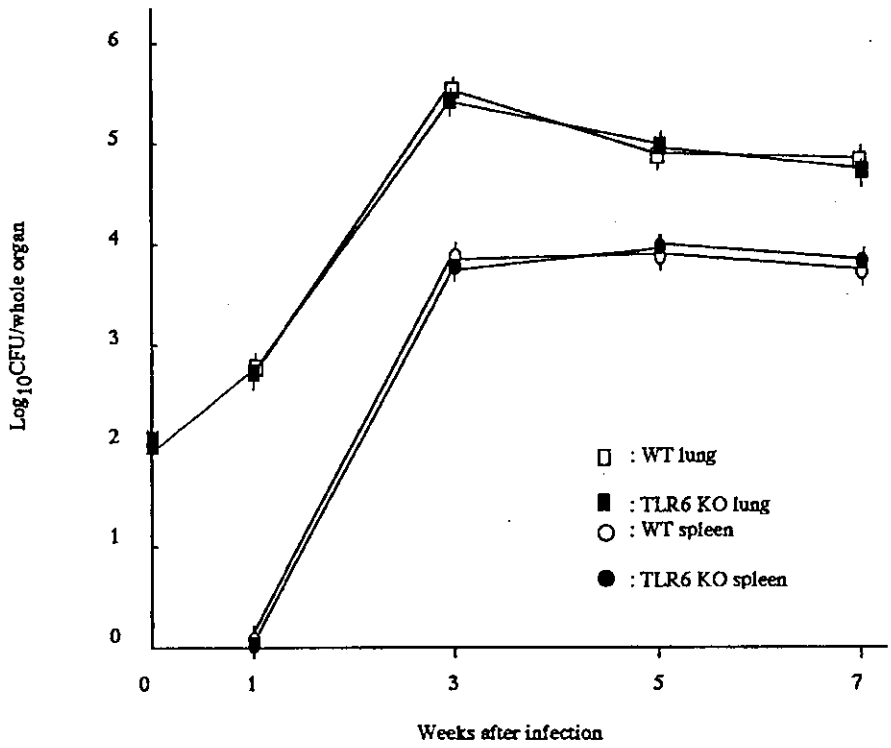

Fig. 2. CFU in lung and spleen tissues of TLR6 KO and WT mice (12 mice each) exposed to 10^6 CFU of *M. tuberculosis* Kurono strain by the airborne route. Error bars indicate standard deviations (SD) of the means.

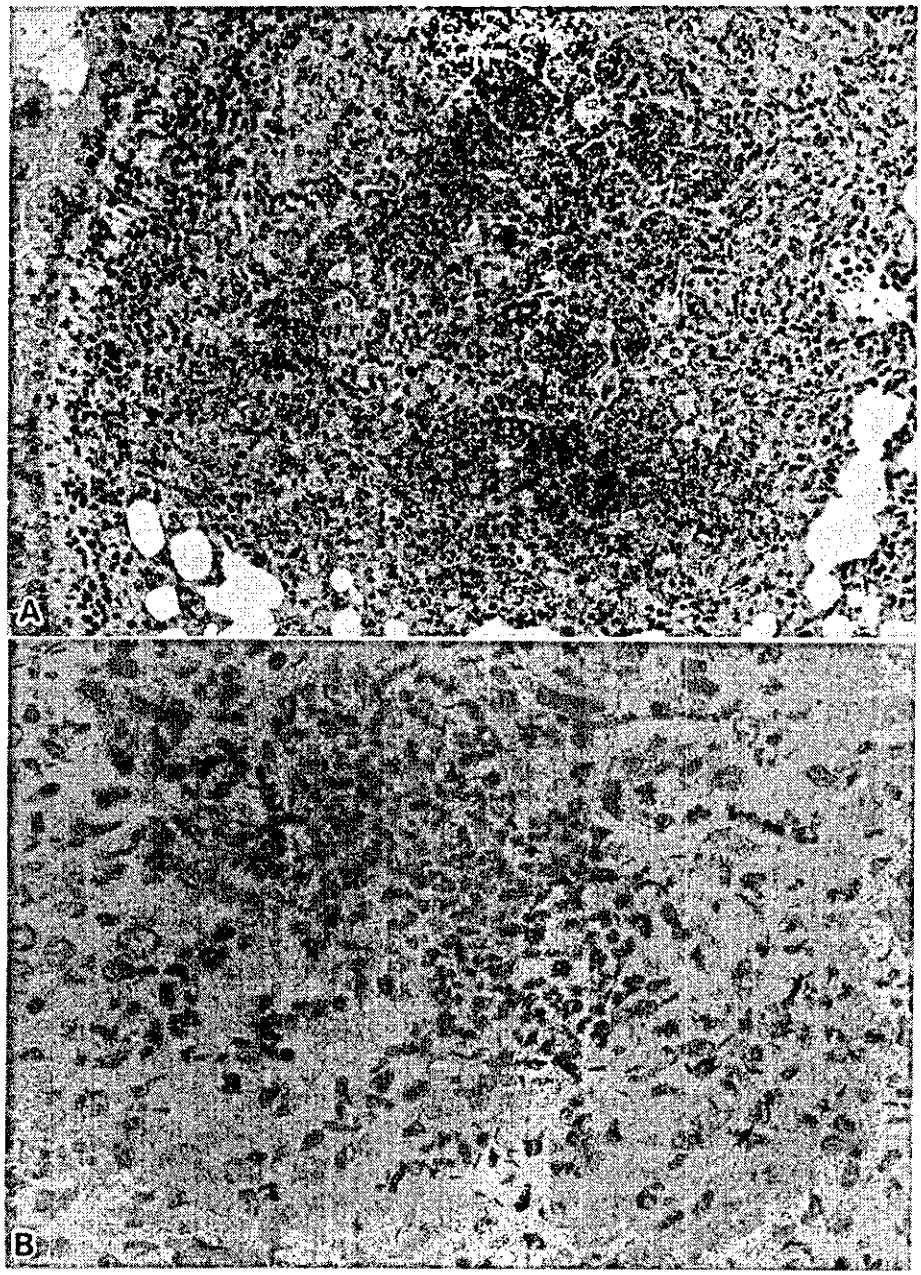

Fig. 3.

20NM (containing 8% formaldehyde and 20% methanol; Wako Pure Chemical Co., Osaka, Japan), dehydrated with a graded ethanol series, treated with xylene, and embedded in paraffin. Sections 5 μm thick were cut from each paraffin block and stained with either hematoxylin and eosin or Ziehl-Neelsen for acid-fast bacilli.

For electron microscopy, the right upper lobe of the lung was fixed with 2.5% glutaraldehyde in 0.1 M phosphate buffer (pH 7.4, PB) at 4 C overnight, washed three times with cold PB, post-fixed with 1% osmium tetroxide in PB at 4 C for 1 hr, dehydrated with a graded acetone series and finally embedded with Spurr's low-viscosity resin (30). Ultrathin sections were obtained with a Reichert Ultracut microtome and stained with uranyl acetate and Sato's lead solution. The stained ultrathin sections were examined with a JEOL 1200EX electron microscope (JEOL, Tokyo).

Electrophoretic mobility shift assay (EMSA) using NF-κB probes. The lung tissues isolated 1 and 5 weeks after aerosol infection and frozen in liquid nitrogen were broken with a hammer between layers of aluminum foil, then transferred to a mortar and reduced to powder in liq-

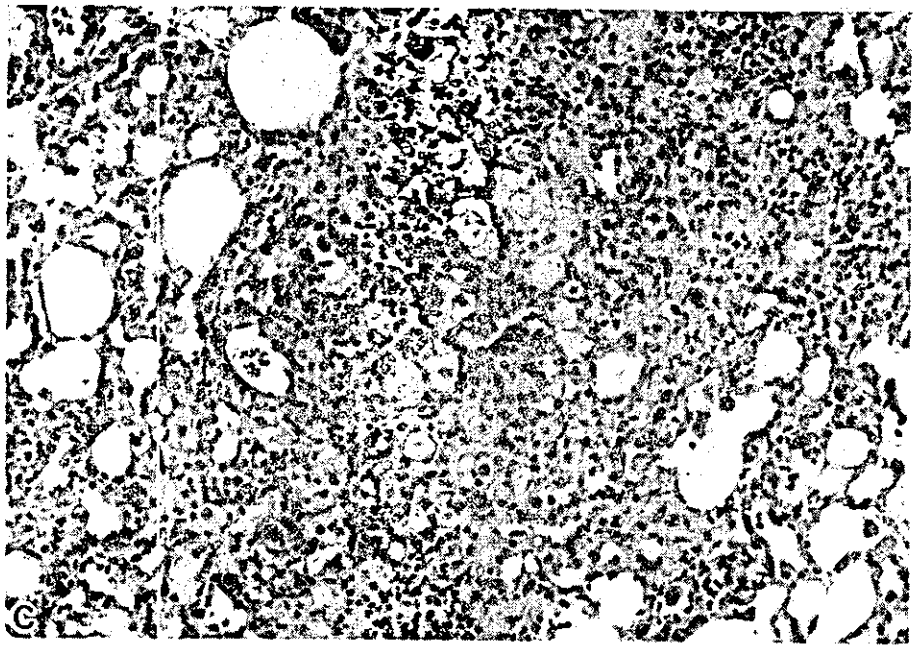

Fig. 3. Histologic examination of the infected lung tissues. Mice were sacrificed 3 weeks after infection, and formalin-fixed sections were stained with hematoxylin and eosin (A and C) and Ziehl-Neelsen for acid-fast bacilli (B). (A) Pulmonary tissue from a TLR2 KO mouse infected with Kurono strain. A large, discrete granulomatous lesion with neutrophil infiltration is recognized. Magnification, ×100. (B) Pulmonary tissue from a TLR2 KO mouse infected with Kurono strain. Many acid-fast bacilli are recognized in the granulomatous lesion by Ziehl-Neelsen staining. Magnification, ×600. (C) Pulmonary tissue from a WT mouse infected with Kurono strain. A discrete granulomatous lesion is recognized. Magnification, ×100.

uid nitrogen. The thawed powder was homogenized in 5 ml of solution A (0.6% NP40, 150 mM NaCl, 10 mM HEPES, pH 7.9, 1 mM EDTA, 0.5 mM phenylmethylsulfonyl fluoride). The supernatant containing the DNA-binding proteins was then divided into small fractions, frozen in liquid nitrogen and stored at −80 C (10). The electrophoretic mobility shift assay using NF-κB and AP-1 probes (Promega) was performed as described previously (26). The specificity of binding was also examined by competition with the unlabeled oligonucleotide.

Statistical methods. Values were compared by Student's *t* test. The level of significance was calculated between groups and by nonparametric equivalents of ANOVA (analysis of variance) for multiple comparison. All animal experiments were performed twice, and the data are presented as cumulative results of all experiments performed.

Results

Mycobacterial Burden in the Lungs and Spleens of TLR2 KO Mice

Both TLR2 KO and C57BL/6 WT mice survived the entire 12-week experimental period. The numbers of tubercle bacilli recovered from the lung and spleen tissues of infected animals after aerosol infection are shown as CFU in Fig. 1. At 1 week after infection, tubercle bacilli were recovered only from the lung tissues of TLR2 KO and WT mice. However, by 3 weeks after infection, the mycobacterial load in the lungs had increased in TLR2 KO mice ($P<0.01$). At 5, 7, and 12 weeks after infection, the bacterial load decreased slightly. Both the TLR2 KO and WT mouse groups showed similar patterns of bacterial growth in the spleen tissues. On the other hand, in WT mice, the bacterial load in both the lung and spleen tissues reached a peak at 5 weeks after infection, and there was no major change in the bacterial load after 12 weeks. As shown in Fig. 2, there was no statistically significant difference in pulmonary CFU counts between TLR6 KO and WT mice.

Light and Electron Microscopic Observation of Infected Lungs

In accordance with the changes in bacterial load, histopathological findings obtained from TLR2 KO and WT mice showed similar changes at 5, 7, and 12 weeks after infection, but at 3 weeks after infection TLR2 KO mice showed large discrete granulomas with neutrophil infiltration (Fig. 3A). No neutrophil infiltration was observed in the pulmonary granulomas of WT mice

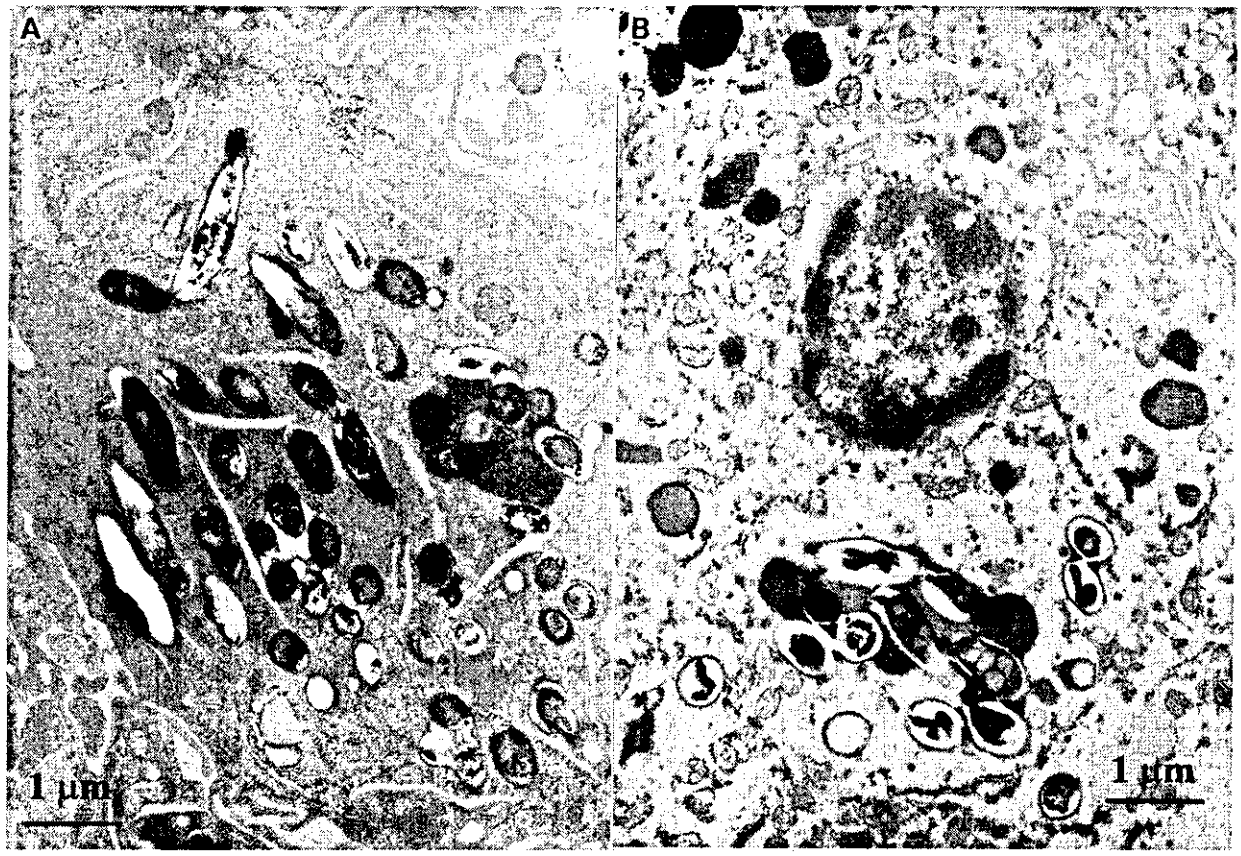

Fig. 4. Electron micrographs of the lung tissues from TLR2 KO (A) and WT (B) mice infected with Kurono strain, obtained 3 weeks after airborne infection. Magnification, ×14,500. Phagosomes (A) ingesting many tubercle bacilli are more prominent in the TLR2 KO mouse (A) than those from the WT mouse (B).

(Fig. 3C). In TLR6 KO mice, pulmonary granulomas were discrete and no significant difference was found in granuloma number and sizes between TLR6 KO and WT mice ($P<0.01$). Electron microscopy revealed that alveolar macrophages in TLR2 KO mice phagocytosed more tubercle bacilli and that the engulfed tubercle bacilli were located in phagosomes (Fig. 4). Tubercle bacilli in the phagosomes of macrophages were relatively long and contained many large vacuole-like structures.

RT-PCR Analysis

Because the mycobacterial CFU assay and histopathological examination indicated that TLR2 KO mice were more susceptible to *M. tuberculosis* than were WT mice, RT-PCR was performed to compare the expression levels of the mRNAs for major cytokines, TGF-β, and iNOS in the lung tissues of TLR2 KO mice with those in lung tissues of WT mice. Figure 5 shows the results of RT-PCR in the infected lung tissues at 1, 3, 5, 7, and 12 weeks after aerial infection. Expression of TNF-α, TGF-β, IL-1β, IL-2, and iNOS mRNA in TLR2 KO mice was significantly lower than that in WT mice until 7 weeks after infection. IFN-γ mRNA expression was slightly lower than that in WT mice. From 5 weeks after infection onward, the expression level of IL-12 p40 mRNA was reduced compared with that of WT mice. On the other hand, expression of IL-10 and IL-18 mRNAs in TLR2 KO mice was similar to that in WT mice. The level of expression of IL-4 and IL-6 mRNAs in the two groups was reversed, because the amplified band of RT-PCR product was more intense in TLR2 KO mice than in WT mice from 3 weeks after infection until 5 weeks after infection. No significant difference was recognized in cytokine mRNA expression between TLR2 KO and WT mice at 12 weeks after infection.

Electrophoretic Mobility Shift Assay (EMSA)

In order to detect DNA binding to NF-κB and AP-1, the nuclear proteins were isolated from the infected lung tissues of TLR2 KO and WT mice at 1 and 5 weeks after infection (10). Samples containing 10 μg of nuclear extract were loaded onto a 4% polyacrylamide gel and run at 120 V for 2 hr. Each gel was then dried and